American Journal of Engineering Research (AJER)
e-ISSN: 2320-0847 p-ISSN : 2320-0936
Volume-6, Issue-8, pp-22-33
www.ajer.org
Research Paper Open Access

Fractal Description of Cloud Drops and Distribution According To Their Sizes

*José Roberto Mercado-Escalante[1], Pedro Antonio Guido-Aldana[2]
[1](Independent Researcher, Mexico)
[2](Professional Development and Institutional Coordination, Mexican Institute of Water Technology,Mexico)
CorrespondingAuthor: José Roberto Mercado-Escalante

ABSTRACT: Clouds are complex dynamical structures in turbulent motion and consist of small droplets that result from water vapor condensation. Inside the cloud, the air between droplets could be saturated or unsaturated. Mixing contributes with an interest mass and energy transfer process: drops provide moisture to the atmosphere while absorbing heat, and change its size. Turbulence motions at different scales could be observed. Gravitation and buoyancy force give rise to convective cells characterize by isotropic or anisotropic turbulence. Despite recent advances in cloud physics, the understanding of key issues such as spatial distribution of cloud drops, turbulence and microphysics interaction, turbulent mixing and size change is far from being complete. The main purpose of this paper is to do a fractal description of the size of a cloud drop by means of different physical laws (Henry 1803, Raoult 1884, van't Hoff 1887) and Cantor process. Distribution of cloud drops by drop size is proposed considering geometric aspects and probability distributions functions.

Keywords: Cloud drops, droplet distribution, cloud microphysics, two phase flow, cloud interface

---

Date of Submission: 11-07-2017 Date of acceptance: 10-08-2017

I. INTRODUCTION

In our latitudes clouds formation process begins with strong winds that raise dust from dry soils by the absence of rain, accompanied by a strong sun that intensifies evaporation and places in the atmosphere increasing amounts of water vapor that seek the encounter with dust particles as condensation nuclei for the growing formation of cloud drops. That happy, contradictory and random encounter between water vapor and particles gives rise to drops of clouds, and within particles or condensation nuclei we emphasize salt. From winds we highlight those that are described as convective that raise potential solutes until heights cold enough for their encounter with water vapor. Condensation releases more and more amounts of heat that feeds winds and places air in turbulent movements that move vapor and solutes in a random way, modifying temperatures scalar field.Our three protagonists are subject to the interaction with the gravitational field, winds hydrodynamic turbulence and electrical interaction between solutes and solvents charges and dipoles. At macroscopic scales, they are subject to interaction with pressure scalar fields, temperature, volume, entropy and composition. Within this context, we should consider the drop of a solution and then get the abstraction of the pure drop of water. As solute we think about salt: sodium chloride, because it is a feasible condition on high seas, being far enough away from the pollution of a city, although due to results we can extend them to other types of solutes.

Drop shape result of doing surface efficient against volume. The drop has a water vapor cover and we express the free energy change due to vapor condensation on liquid surface. We do a transformation in a rectangular volume separated by a semipermeable porous partition, which allows water to pass but retains the solute. In the transformed analogous volume, two heights are equal, expressing the equilibrium of the two parts.In order to carry out a detailed analysis to get a fractal description of drops of clouds, we should considerer at first thermodynamic potentials and perform Legendre transformations that allow us to generate new potentials by changing a state variable at each step. We identified possible variables of the multi-fractal description and found the associated spectra. Two integers representing surfaces and volumes dimensions and their ratio emerges prominently, which we interpret as the ratio of the surface energy, which also can be interchangeable, against all the energy reserve contained in its volume. We recall different physical laws [1], [2] and [3], to take into account scalar fields composition, to quantify changes in potentials, and to represent them by means of

usual and appropriate physical parameters. We do a Cartesian product of Cantor processes that allows us to build a possible size distribution. Also, we do a double inversion of the circle and sustained our results with data reported by [4]. We think of a Poisson random variable with its only parameter linked to the relative spatial frequency of solute moles number. Next, we think of a discrete Pascal random variable or negative binomial identifying success probability. Then we consider an Erlang distribution with its parameters: spatial and events. Finally, we state the Gamma continuous random variable and its two parameters linked with physical magnitudes reported by Legendre transformations and solutions laws. Results are graphed based on data reported by [4]. Besides we discussed other results and state our main conclusions.

II. MATHEMATICAL APPROACH

In this section, a mathematical approach to do a fractal description of a cloud drop and its size probability distribution is presented. We imagine our three main protagonists in a scalar field of pressure, temperature, volume, entropy and composition. The main potential is the internal energy in state variables: entropy *S* and volume *V*. But in real systems, it is generally difficult to maintain entropy constant, since this implies a good thermal insulation. It is therefore more convenient to start out from the Helmholtz free energy *F* as a function of temperature *T* and volume *V*. Since Helmholtz free energy is determined by two variables, temperature *T* and volume *V*, two Legendre transformations can occur: in the first one, volume *V* is changed by pressure *P* and Gibbs potential is obtained, with state variables, temperature *T* and pressure *P*. In the second, temperature *T* is changed by entropy *S* and the internal energy *E* emanated in state variables, entropy *S* and volume *V*. However, laboratory experiments are often carried out under constant pressure and temperature conditions, so Gibbs potential is adequate:

$$F(T,V) \mapsto \begin{cases} \Phi(T,P) = F + VP, & V \mapsto P \\ E(S,V) = F + TS, & T \mapsto S \end{cases} \tag{1}$$

We assume that a drop is formed by vapor molecules condensation, so there are two phases: saturated water vapor and liquid water. Consequently, the system has another state variable, the composition, and we must replace pressure variable by composition variable by means of a new Legendre transformation, therefore we obtain Gibbs potential in temperature and composition variables.The system is supposed to be closed at a certain temperature, droplet of specific radio contains a definite molecules number and in both vapor and liquid phases, chemical potentials are known per molecule. Gibbs potential change is calculated by an increase in the liquid phase area with the realization of a certain amount of work by surface tension and chemical potentials change between states: vapor and liquid. The first change is specified by $4\pi r^2 \sigma_{lv}$ and the second by $-(\Delta\mu_{vl})\alpha$, therefore change is:

$$\Delta G = 4\pi r^2 \sigma_{lv} - (\Delta\mu_{vl})\alpha \tag{2}$$

Where $(r, \sigma_{lv}, \alpha, \Delta\mu_{vl} = \mu_v - \mu_l)$ are: droplet radius, surface tension coefficient, molecules number in the drop and chemical potentials change of vapor minus liquid.

2.1 Analysis of the solution

We recall that [2] can be enunciated as a contraction of saturated vapors pressure with respect to pure solute pressure. And there is an analogous expression for solvent. Contraction factor is the molar fraction or relative frequency of moles number, $\nu_i / \nu_1 + \nu_2$, for solute *i = 1*, for solvent *i = 2*, being pressure in solution less than the pressure in the pure state: $p_i < p_i^{(0)}$. In addition, for real gases, solute pressure presents an additional reduction, so there is an aggregate contraction factor according to[1], so solute pressure in solution is p_1 / ι, which would be equivalent to an apparent increase of solute molar fraction: $\nu_i / \nu_1 + \nu_2$ changes to $\iota(\nu_i / \nu_1 + \nu_2)$, and we obtain: $p_1 = \iota(\nu_i / \nu_1 + \nu_2) p_1^{(0)}$, being ι the van't Hoff factor, which depends on solute chemical nature and dissociation degree (a known value for salt is 2.7), [5].

Finally, we remember that for diluted solutions, we count on van'tHoff [3], which states that, $p_{osm} = \ln\left(1 + \iota \frac{\nu_1}{\nu_1 + \nu_2}\right) \frac{RT}{V_M}$, being ν_i the solute moles number, *i = 1*, or the solvent moles number, water, *i = 2*,

and ι the van't Hoff factor. Work could be expressed by $p_{osm}\, dV = \frac{dm}{\rho'_L} \ln\left(1 + \iota \frac{\nu_1}{\nu_1 + \nu_2}\right) \frac{RT}{V_M}$ or either $p_{osm}\, dV = kT \frac{\rho_l}{\rho'_l} \ln\left(1 + \iota \frac{\nu_1}{\nu_1 + \nu_2}\right)$.

On the other hand, work by surface tension is $\frac{\sigma' / kT}{A} \frac{dA}{dr} \frac{dm}{\rho'_l}$ that produces: $2 \frac{\sigma'}{kT} \frac{M_a / N_0}{\rho'_l} \frac{1}{r}$. An additional variation of the original free energy is the reduction that is evaluated by osmotic pressure work: $kT \ln\left(1 + \iota \frac{\nu_1}{\nu_1 + \nu_2}\right)^{-\frac{\rho_l}{\rho'_l}}$. If p is the pressure of the supersaturated vapor and p_∞ the vapor pressure in equilibrium at temperature T on a liquid flat surface, the change by drop condensation is $\Delta\mu_{vl} = kT \ln S$ with $S = p / p_\infty$. Therefore, total change in thermal energy units is,

$$2 \frac{\sigma'}{kT} \frac{M_a / N_0}{\rho'_l} \frac{1}{r} + \ln\left(1 + \iota \frac{\nu_1}{\nu_1 + \nu_2}\right)^{-\frac{\rho_l}{\rho'_l}} = \ln S \tag{3}$$

The first transformation performs from the previous expression (3), is to rewrite the three terms of the free energy change as: $\ln \frac{p}{p_\infty} = A' \frac{1}{r} + \ln\left(1 + \iota \frac{\nu_1}{\nu_1 + \nu_2}\right)^{-\frac{\rho_l}{\rho'_l}}$, with $A = \frac{2\sigma'}{RT} \frac{M_a}{\rho'_l}$, and then obtain a representation of the surface tension work contribution in the form: $\ln \frac{p / p_\infty}{\left(1 + \iota \frac{\nu_1}{\nu_1 + \nu_2}\right)^{-\frac{\rho_l}{\rho'_l}}} = A \frac{1}{r}$

In the multifractal description called "*strange attractor*" [6] and [7], we assume Gibbs free energy change as a structure function, in thermal energy units. Scale variable is identified by the change in the chemical potential occurring in condensation $s = \Delta\mu_{vl} / kT$, also in thermal energy units; singularity, being molecules average number in the drop in solution; and spectrum, represented by the work done by surface tension, in thermal energy units:

$$\tau(s) = f(\alpha(s)) - s\alpha(s) \tag{4}$$

Solution volume is writing as: $V_1 + V_2 = \frac{(M_1 / N_0)\alpha_1 + (M_2 / N_0)\alpha_2}{\rho'_l}$, or $V_1 + V_2 = \frac{\tilde{\alpha}}{N_0} \frac{M_1 + M_2}{\rho'_l}$. Surface tension work by drop condensation can also be written as $\sigma' dA = \sigma' \frac{dV}{dr} = 4\pi r^2 \sigma'$, per thermal energy unit, and in terms of molecules average number is: $3\left(\frac{4}{3}\pi\right)^{1/3} \left(\frac{1}{N_0} \frac{M_1 + M_2}{\rho'_l}\right)^{2/3} \frac{\sigma'}{kT} (\tilde{\alpha})^{2/3}$

Spectrum is: $f(\tilde{\alpha}) = C_{12} (\tilde{\alpha})^{2/3}$ where $C_{12} = 3\left(\frac{4}{3}\pi\right)^{1/3} \left(\frac{1}{N_0} \frac{M_1 + M_2}{\rho'_l}\right)^{2/3} \frac{\sigma'}{kT}$. Spectrum maximum condition gives: $\frac{2}{3} \frac{C_{12}}{\tilde{\alpha}^{1/3}} = s$ and by inverting the singularity in terms of the radius: $\tilde{r} = \frac{2}{3} C_{12} \frac{\left(\frac{1}{N_0} \frac{M_1 + M_2}{\rho'_l}\right)^{1/3}}{\left(\frac{4}{3}\pi\right)^{1/3}} \frac{1}{s}$, which produces:

$$\tilde{r} = \frac{2\sigma'}{RT}\left(\frac{M_1 + M_2}{\rho'_l}\right)\frac{1}{s}, \quad s = \ln \frac{p/p_\infty}{\left(1 + \iota \frac{\nu_1}{\nu_1 + \nu_2}\right)^{-\rho_l/\rho'_l}}, \tag{5}$$

In the very dilute case, solute moles number is very small relative to solvent or water, whereby solute molar fraction tends to zero and composition is reduced to pure water:

$$r_p = \frac{2\sigma_{lv}}{RT}\left(V_{M_2}\right)\frac{1}{s}, \quad s = \ln\, p/p_\infty, \quad V_{M_2} = \frac{M_2}{\rho_l} \tag{6}$$

where it is observed that drop radius is proportional to surface energy and water molar volume, while it is inversely proportional to relative humidity logarithm, results known by [8] and [9]. Of course we also have the possibility to develop the fractal model for pure water drop. For this we express drop radius in terms of its volume, and this in terms of drop molecules number, and then obtain the work, in thermal energy units and in terms of molecules number α.

Scale variable in this multifractal description is also the chemical potential change occurring in the condensation $s = \Delta\mu_{vl}/kT$, in units of thermal energy; the singularity is the number of molecules in the drop α, spectrum represents the work done, in thermal energy units. And the structure function $\tau(s)$ is also the change in Gibbs free energy potential, in thermal energy units:

$$\tau(s) = C(\alpha(s))^{2/3} - s\alpha(s), \quad f(\alpha) = C(\alpha)^{2/3}, \quad s = \Delta\mu_{vl}/kT \tag{7}$$

Thus we have the expression for droplet radius in terms of relative humidity and proportional to the length A_0, which represents surface tension or energy per unit area on the surface, temperature, and water density ratio to its molecular weight; is the ratio of the number of moles contained in the drop to the volume of the drop:

$$r = \frac{1}{\ln S}A_0, \quad A_0 = \frac{2\sigma_{lv}}{RT}V_{M_a}, \quad V_{M_a} = \frac{M_a}{\rho_l}, \quad S = \frac{p}{p_\infty} > 1 \tag{8}$$

2.1.1 The critical radius

Of the three contributions to the Gibbs energy potential change, we do an approximation in the expression of osmotic pressure work. Molar fraction term $\iota\frac{\nu_1}{\nu_1+\nu_2}$ is approximated by $\iota\frac{\nu_1}{\nu_2}$, then by $\iota\frac{M_2}{M_1}\frac{m_1}{\left(\frac{4}{3}\pi r^3\rho'_l - m_1\right)}$, next by $\frac{3}{4\pi}\frac{M_2}{\rho'_l}\left(\iota\frac{m_1}{M_1}\right)\frac{1}{r^3}$. So the term: $\ln\left(1+\iota\frac{\nu_1}{\nu_1+\nu_2}\right)^{-\frac{\rho_l}{\rho'_l}}$ is approximated by, $-\frac{\rho_l}{\rho'_l}\frac{3}{4\pi}\frac{M_2}{\rho'_l}\left(\iota\frac{m_1}{M_1}\right)\frac{1}{r^3}$ and finally by: $-B\frac{1}{r^3}$, $B = \frac{3}{4\pi}\frac{\rho'_l}{\rho_l}\frac{M_2}{\rho'_l}\left(\iota\frac{m_1}{M_1}\right)$. Thus three contributions are now: $A\frac{1}{r}$, $-B\frac{1}{r^3}$ and $\ln\frac{p}{p_\infty}$. So we obtain $A\frac{1}{r} - B\frac{1}{r^3} = \ln S$. Humidity has one extreme in $r = r_c = \left(\frac{3B}{A}\right)^{1/2}$ which it is called "critical radius".

2.1.2 Inversion in a circle

Now we do an inversion transformation on a sphere. Sphere radius is symbolized by r_δ . Its value is mean proportional between critical radius and the distance between mean radius and critical radius, $\frac{r_c}{r_\delta} = \frac{r_\delta}{\bar{r} - r_c}$, $\bar{r} = \delta r_c$. But it is also average proportional between two distances $\frac{R}{r_\delta} = \frac{r_\delta}{r}$; therefore, $\frac{R}{\bar{r} - r_c} = \frac{r_c}{r}$, $\bar{r} = \delta r_c$ with $\delta > 1$. We perform a displacement by the value r_0, the minimum value of r, and find $\frac{R}{\bar{r} - r_c} = \frac{r_c - r_0}{r - r_0}$. Finally, with $l_a = r_c - r_0$, $\gamma = 1/(\bar{r} - r_c)$ we obtain: $R = \frac{l_a}{\gamma}\frac{1}{r - r_0}$.

An important special case arises when mean radius supplement over the critical radius is the inverse of the mean radius: $\bar{r} - r_c = (\bar{r})^{-1}$ or $\delta - 1 = (\delta)^{-1}$ resulting $\delta = (1 + \sqrt{5})/2$, which corresponds to the well-known gold number structure.

2.1.3 Another representation of work

Changes synthesis in Gibbs free energy potential was expressed through a representation of surface tension work: $\ln \frac{p / p_\infty}{\left(1 + \iota \frac{\nu_1}{\nu_1 + \nu_2}\right)^{-\frac{\rho_l}{\rho'_l}}} = A \frac{1}{r}$, we transform it into $e^{-A\frac{1}{R}} = \frac{100}{H}\left(1 + \frac{\rho'_l}{\rho_l} B \frac{1}{R^3}\right)^{-\rho_l/\rho'_l}$, which in turn is $e^{-A\frac{\gamma}{l_a}(r - r_0)} = \frac{100}{H}\left(1 + \frac{\rho'_l}{\rho_l} B \left(\frac{\gamma}{l_a}\right)^3 (r - r_0)^3\right)^{-\rho_l/\rho'_l}$, and the exponent $b = \frac{\rho_l}{\rho'_l} < 1$. To limit the right side we need to reinforce the exponent *b* through a dilation; we do this by multiplying by the factor *n> 1* and find $e^{-nA\frac{\gamma}{l_a}(r - r_0)} = \left(\frac{100}{H}\right)^n \left(1 + \frac{\rho'_l}{\rho_l} B \left(\frac{\gamma}{l_a}\right)^3 (r - r_0)^3\right)^{-n\rho_l/\rho'_l}$. In addition, we multiply by $(r - r_0)^m$, appropriately choose the variable to obtain $u^{m/3}(1 + u)^{-nb}$, we bound by means of an integration in the variable $t = \frac{u}{1 + u}$, which produces the Euler Beta function $B(m/3 + 1, nb - m/3 - 1)$, on condition that $nb > m/3 + 1$, which is obtained if *n* is sufficiently high [10]. This exponent expansion factor is provided by the ratio of critical radius to drop characteristic length l_a / A, which, for the present case, runs several orders of magnitude from 10^2 to 10^6, which can be seen in Table 1, thus fulfilling well for the purpose of dilating the exponent *b*.

We return to Gibbs potential changes expression: the expression $(r - r_0)^m e^{-nA\frac{\gamma}{l_a}(r - r_0)}$ has, as already said, an integral bounded by the Euler Beta function; we normalized it and obtained $\frac{\gamma^\alpha}{\Gamma(\alpha)}(r - r_0)^{\alpha - 1} e^{-\gamma(r - r_0)}$ with $\alpha - 1 = \gamma l_a, \quad \gamma = \lambda \frac{A}{l_a}, \quad \alpha > 0, \gamma > 0$. Euler Beta function $B(m/3 + 1, nb - m/3 - 1)$ is produced with $p = \frac{u}{1 + u}$ which represents the success probability; its inverse $u = \frac{p}{1 - p}$ symbolizes the ratio of success probability with respect to that of failure. The magnitude *u* is derived from the contraction in solute pressure in solution state with respect to the same in pure state, reinforced with the additional contraction that is enunciated in Henry's law for real gases which produce the contraction factor $\iota \frac{\nu_1}{\nu_1 + \nu_2}$, which we can approach to $\iota \frac{\nu_1}{\nu_2}$.

If we think of a Poisson random variable with its only parameter representing the contraction factor $\iota \frac{\nu_1}{\nu_1 + \nu_2}$ and given by $\mu = \frac{a_0}{\bar{r}} = \frac{a_0}{\delta r_c} = \frac{p}{1 - p}$ with $p < 1, n > 1, \quad \delta = \frac{n}{n - 1}$, we have that success probability is determined by the inversion $p = \frac{\mu}{1 + \mu} = \frac{1}{1 + \delta(r_c / a_0)}$. Then an Erlang random variable could be considered with the first parameter continuous and the second discrete $\lambda = n\mu = n\frac{p}{1 - p}, \quad n = \alpha$ with $p < 1, n > 1, \quad \delta = \frac{n}{n - 1}$, or the Gamma with the continuous parameters $n = \frac{\delta}{\delta - 1}, \quad \delta > 1$.

Then the contraction of Raoult and Henry laws are expressed in the Poisson parameter $\mu = \frac{a_0}{\delta r_c} = a_0 \frac{n - 1}{n}\left(\frac{A}{3B}\right)^{1/2}$ and $n > 1$. In the Erlang variable, it is manifested in the two parameters

$\lambda = n\mu = a_0(n-1)\left(\frac{8\pi}{9}\frac{\sigma'}{R_g T}\frac{\rho'_l}{\rho_l}\frac{M_1}{\imath m_1}\right)^{1/2}$ and $\alpha = n > 1$. Parameters physical content of distributions are summarized in (9),

$$\frac{\mu}{a_0} = \frac{n-1}{n}\left(\frac{A}{3B}\right)^{1/2}, \quad \frac{\lambda}{a_0} = (n-1)\left(\frac{8\pi}{9}\frac{\sigma'}{R_g T}\frac{\rho'_l}{\rho_l}\frac{M_1}{\imath m_1}\right)^{1/2}, \quad \alpha = n > 1 \tag{9}$$

Once parameters of probability distribution density have content based on physical quantities, we re-find Gamma distribution by means of a generalized Cantor process, as a proposal of probability density for drops diameters, which is supported by known experimental results.

It is chosen as features basis $f(q) = 1/(1+q)$ and the succession $P_n = (-1)^n \partial_q^{(n)}(1/(1+q))\cdot(n+1)\partial_p^{(-n)}(p)\Big|_q$ is calculated, which produces $P_{2n} = (1+1/q)^{-(n+1)}$, we discretized by introducing resolutions sequence $q_n = n/\lambda y$, and considering the limit results $P_2 = e^{-\lambda y}$. Analogously with $f(h) = h^{-\alpha}, h > 1, \alpha > 0$ the following equivalence is finally obtained $P_1 = \frac{x^{\alpha-1}}{\Gamma(\alpha)}$. For the product, from some *n* it is presented that $x = y = \phi$, and with the normalization or conservation of the probability one obtains: $\lambda^\alpha \frac{\phi^{\alpha-1}}{\Gamma(\alpha)} e^{-\lambda\phi}$, or $\frac{\lambda^\alpha}{\Gamma(\alpha)}\left(\frac{x}{a_0}\right)^{\alpha-1} e^{-\lambda\left(\frac{x}{a_0}\right)}$, [11] and [12].

Alternatively, unit *1*, as success certain, supports Laplace's inverse transform representation: $1 = \ell^{-1}\left(\frac{1}{s}\right)$, and for n success: $1*1*\cdots*1 = \ell^{-1}\left(\frac{1}{s}\right)*\ell^{-1}\left(\frac{1}{s}\right)*\cdots*\ell^{-1}\left(\frac{1}{s}\right) = \ell^{-1}\left(\frac{1}{s}\cdot\frac{1}{s}\cdot\ldots\cdot\frac{1}{s}\right)$, so that: $(1*1*\cdots*1)(t) = \frac{t^{n-1}}{\Gamma(n)}$, is obtained $\ell^{-1}\left(\frac{1}{s^n}\right)(t) = \frac{t^{n-1}}{\Gamma(n)}$, and with the slipping property results: $\ell^{-1}\left(\frac{1}{(\lambda+s)^n}\right)(t) = \frac{t^{n-1}}{\Gamma(n)}e^{-\lambda t}$; and after normalizing a random variable of Erlang is obtained $\frac{\lambda^n}{\Gamma(n)}t^{n-1}e^{-\lambda t}$.

A connection with the differential equations is stablished. For one success $n = 1$, $\ell^{-1}\left(\frac{1}{s+\lambda}\right)(t) = e^{-\lambda t}$ which can be generalized in $\ell^{-1}\left(\frac{s^{\gamma-1}}{s^\gamma+\lambda^\gamma}\right)(t) = E_{1,\gamma}\left(-(\lambda t)^\gamma\right)$, this is the well-known Mittag-Leffler function, solution of the differential equation (10) and from which the exponential is recovered as a special case with $\gamma = 1$,

$$D_t\psi(t) = -\lambda^{-\sigma} D_t^{1-\gamma}\psi(t) \tag{10}$$

The constant $\lambda^{-\sigma}$ depends on the spatial behavior of the phenomenon, so we have two paths: 1. there is no spatial manifestation so it is a constant and we take $\sigma = \gamma$ y $\lambda = t_r$ as reference time or unitary type; and 2. there is spatial manifestation and the equation (12) arises.

In the first case, a solution is expressed by $\psi(t) = E_{1,\gamma}\left(-(t/t_r)^\gamma\right)$, is the Mittag-Leffler function with parameter γ which is shown in (11), [13],

$$E_{1,\gamma}\left(-(t/t_r)^\gamma\right) = \sum_{j=0}^{\infty}\frac{\left(-(t/t_r)^\gamma\right)^j}{\Gamma(1+\gamma\cdot j)} \tag{11}$$

In the second case, $\lambda^{-\sigma}$ could be related with the dual variable to the spatial position that is accustomed to denote $\|k\|^\sigma$, so the term is interpreted as: $\lambda^{-\sigma}\psi(t) \mapsto \|k\|^\sigma \psi(k,t)$, and corresponds to the Fourier transform of the probability density $P(x,t)$, which in turn is the transform of the fractional derivative $D^\sigma_{\|x\|}P(x,t)$, with

changed sign, in its form Riesz derivative: $-F\left(D_{\|x\|}^{\sigma}P(x,t)\right)(k)=\|k\|^{\sigma}\psi(k,t)$. So alternatively (10) stay: $D_t^{\gamma}(1-\psi(k,t))=-F\left(D_{\|x\|}^{\sigma}P(x,t)\right)$, and with the inverse Fourier transform results: $D_t^{\gamma}(-\delta(x)+P(x,t))=D_{\|x\|}^{\sigma}P(x,t)$, which is the fractional Fokker-Planck equation (12), also known as Einstein-Kolmogorov equation [14],

$$D_t^{\gamma}P(x,t)=D_{\|x\|}^{\sigma}P(x,t)+D_t^{\gamma}(1\delta(x)) \tag{12}$$

Therefore, the obtained function $\psi(k,t)\mapsto\psi(t)$ is the characteristic function, with temporal parameter, of the passage or transition probability of the fractional Fokker-Planck equation, with $\sigma=\gamma=1$ and $\lambda=t_r$.

III. DISCUSSION

Evidently, probability density is asymmetric, [15] and [16]. We can inquire under what conditions that quality disappears. For this we calculate asymmetry parameter as the third central moment with respect to the third power of the standard deviation, results: $\frac{2}{\sqrt{\alpha}}$. But this tends to zero only if $\alpha\to\infty$, which as Erlang distribution would turn it into a Dirac delta, but then the critical radius would become zero, which is a physical impossibility because solute's mass would be zero, or else it would be an impossible mathematical due $\delta=1$.

Considering [17], if $\alpha\to 1$ it would be obtained $r_c\to 0$ which is absurd from the physical point of view because it is equivalent to consider if $B\to 0$ we would have $m_1\to 0$ and the drop would be pure water, or if $A\to\infty$ it would imply that $T\to 0$ is reached. But on the other hand, within the two exponents, that of form is the most important, because it is the power of the success probability.

Interaction between turbulence and a generic drop has consequences on droplets size distribution. [18] and [19] explain that as a consequence of the equilibrium expressed in the dynamic quadrilateral formed by: drop weight (as sediment), pressure drag, friction drag and Archimedes' flotation, flotation increases with turbulence increment and reciprocally diminishes with the approach to laminar regime. For example, due droplets evaporation, flotation component may decrease [20]. But also, with turbulence intensification, vortex knots that interact with droplets become smaller and smaller, so that eventually they could reach the Kolmogorov scale of fractions order of 1 mm. Thus a knot could be of a size comparable with that of 10 drops of 10 μm in diameter [21], [22], [17] and [23]. Regarding to [17], fluid Lagrangian acceleration can be translated into an expression of the type $-(1-1/\beta_n)u$, so in the very turbulent regime it approaches to $(1/\beta_n)u$ which constitutes a fluid acceleration dilation that will eventually be more greater than gravity and will result in a predominance of flotation.So evaporation and cooling that accompanies it is produced, as well as a mixture of air with average relative humidity reduction, the first causes an increase of radius r, the second produces another increase at the same radius, so we have a shift towards the right of the parameter, or the lowering of the shape parameter [24] and [25].Now we consider the case of border interface of cloud interior with outside clear air: exterior temperature is slightly higher than that of the interior, and the exterior, with lower relative humidity (sub-saturated), while the interior over-saturated. Imagine an air flow from outside to inside with a mixture of the previous two. Evaporation and also the accompanying cooling is produced, as well as a mixture of air with the reduction of the average relative humidity; the first causes a radius increment, the second causes another increase at the same radius, thus we have a displacement towards the right of the parameter δ, or the decrease of the form parameter α, [24] and [25].

We intend to observe the compatibility of our results with others of experimental order. To do so, we translate them into our context. For example, if we know modal radius and standard deviation by means of the experimental procedure, we determine the quotient $c=(\alpha-1)/\sqrt{\alpha}$, which is inversed and result $\alpha=\left((c/2)+\sqrt{(c/2)^2+1}\right)^2$.

In particular, if the dilation factor δ, which transforms the critical radius into the mean radius, is the "gold number"; we imagine a cloud with the two statistics mentioned equal to unity so that the previous quotient becomes 1, and we get $\alpha=\left((1+\sqrt{5})/2\right)^2$ or either $\lambda=(1+\sqrt{5})/2$. Then its graph looks analogous to the second curve of the group: drops in solution II, which corresponds to the mass of the solute $m_1=10^{-12}\ gr$.

Similarly, from the experimental data published in [26], we can find shape parameters values of the gamma density and judge the compatibility with our results. Of all of them we highlight the case of the Sauter radio 55 μm, from which we obtained the parameter triplet $(\alpha, \lambda, \delta) = (3.08, 0.09, 1.48)$, and which is analogous to one of the group: drops in solution II. In addition, from [27], based on mean value and standard deviation, we obtained: $(\alpha, \lambda, \delta) = (2.45, 0.40, 1.69)$ which is analogous to the second [4] data: $(\alpha, \lambda) = (2.5, 0.5)$.

Another point of discussion is obtained from the fractal description of the drop in solution, because it produces a spectrum that is determined by the exponent $2/3$, which means the ratio of two dimensions: that of the surface energy with respect to the energy of the volume. But these two integers create the number 13 through Fermat's theorem of the representation of congruent primes with 1 in the group of integers module 4, as sum of two squares of integers. But, the number 13 is the number of *"jade"* in the calendar of the ancient Mesoamerican towns, a calendar that can be represented as the Cartesian product of two circles or Toro: the major containing an icosagon and the minor a tridecagon, and which complete a total of 18 months of 20 days each one, covered by various and successive Gods who preside every thirteen days, plus 5 unlucky days, [28].

Distribution density knowledge is also of practical importance in other areas such as agriculture, meteorology, medicine, pharmaceuticals, and other industrial processes such as: combustion, paint sprays, metal powders [29].In the special case of energy towers, where smallwater drops are sprayed into the tower from the top to generate a downward flow of humid air to move wind turbines arranged at the bottom, distribution density is important to understand and characterized drops dynamics and evaporation process [30]. In addition of gamma distribution, normal log and also Rosin-Rammler distribution are used[31].

IV. CONCLUDING REMARKS

- Fractal model for drop in solution is determined by identifying singularities in the medium molecules number in the drop, scales in relative humidity, the spectrum in the work done by the surface tension and the structure in the change of Gibbs potential.
- The ratio of surface size to the volume plays the essential role for the spectrum exponent of both drop in solution and drop of pure water.
- Gamma continuous random variable is determined with the shape parameter determined by the relative distance between mean radius and critical radius and "the passage frequency" by the mean radius. Its physical content is made explicit in (9).
- Gamma density of cloud droplet size distribution can be interpreted as the characteristic function, with temporal parameter, of the passage probability or transition of a fractional Fokker-Planck equation.
- We plot probability densities graphs based on data published by [4], but reorganizing their data as shown in the following two tables. In Table 1 we have data for droplet in solution parameterized with the physical quantities. The solute is salt (NaCl), temperature is 10°C, contraction factor for critical radii is 0.31 from right to left, that is from the highest solute masses to the lowest. In the table, values corresponding to the parameters A and B are represented. With the first three values sets for alpha and lambda, from left to right, the graph is doing: Drop in solution I; with the following three: Drop in solution II, and with the last three: Drop in solution III.

Table 1. Data for droplet in solution parameterized with the physical quantities.

		Na = 11	**Cl = 17**	**NaCl**	**A=3.2*10^-5/T**	**Contraction Rc**			
		22.9898	35.453	58.4428	283	0.316227766			
					0.001130742				
B=8.6*(m1/M1)	1.4715E-05	0.00014715	0.00147152	0.01471524	0.147152429	1.471524294	14.71524 29	147.1524 29	1471.5242 9
m1 (g)	1E-16	1E-15	1E-14	1E-13	1E-12	1E-11	1E-10	1E-09	0.00000001
Critical radius Rc (μm)	0.19758891	0.62483101	1.97588914	6.24831009	19.7588914	62.48310085	197.5889 14	624.8310 09	1975.8891 4
alpha	3.14358881	2.9487171	2.771561	2.61051	2.4641	2.331	2.21	2.1	2
lambda	10.8487302	3.11879064	0.89658927	0.25775129	0.074098287	0.02130176	0.00612383	0.00176048	0.0005061
delta	1.46650738	1.51315812	1.56447393	1.62092132	1.683013455	1.751314801	1.82644628	1.90909091	2

Note: The greatest number of decimals was considered

In Table 2, we have the field data also published by [4] and reorganized according to the inversion in the circle.

Table 2. Field data also published by [4] and reorganized according to the inversion in the circle.

		rmin	r50	rc	rm	rmax	lambda	alpha	delta
Small continental cumulus (Cu)									
USA		3		6	9	33	0.33333333	2	1.5
Small maritime cumulus (Cu)									
Hawaii		2.5	12	11	15	20	0.25	3.125	1.36363636
Cumulus congestus	"Cauliflower" 6km Base 0.6 K								
USA		3		6	24	83	0.05555556	1.16666667	4
Cumulonibus (Cb)									
USA		2		5	20	100	0.06666667	1.2	4
Altostratus (As)	2km to 7km								
Germany		1		4.5	5	13	2	8	1.11111111
Nimbostratus (Ns)	0 to 2km								
Germany		1		4	6	20	0.5	2.5	1.5

In the following figures the distribution of cloud drops by drop size is present considering: Fig. 1, data of [4]; Fig. 2, Droplet in solution I; Fig. 3, Droplet in solution II; Fig. 4, Droplet in solution III.

Alpha	8 (Blue)	2.5 (Magenta)	3.125 (Green-Blue)	9.23 (Light Green-Blue)
Lambda	2 (As)	0.5 (Ns)	0.25 (Cu)	0.55

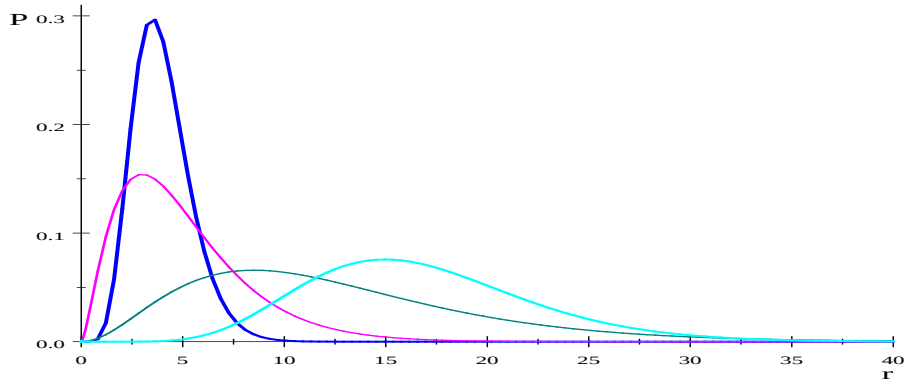

Figure 1. Distribution of cloud drops by drop size with data of [4].

Alpha	3.14 (Blue)	2.94 (Magenta)	2.77 (Bluish green)
Lambda	10.9	3.11	0.9

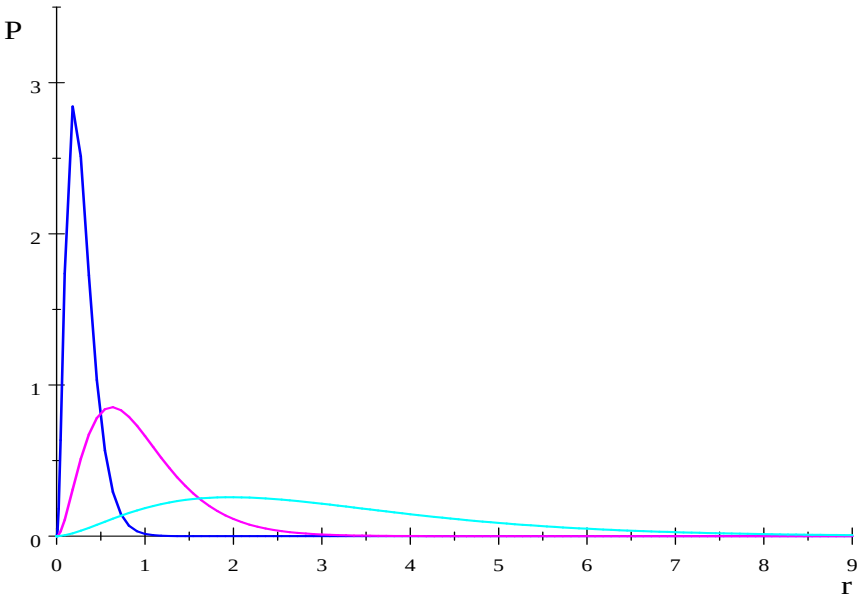

Figure 2. Distribution of cloud drops by drop size considering droplet in solution I.

Alpha	2.61 (Blue)	2.46 (Magenta)	2.33 (Bluish green)
Lambda	0.26	0.07	0.021

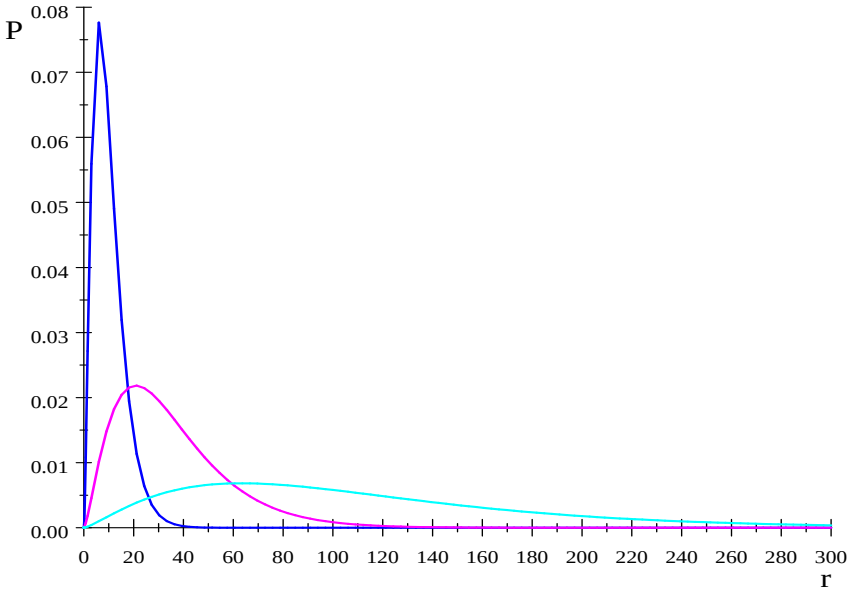

Figure 3. Distribution of cloud drops by drop size considering droplet in solution II.

Alpha	2.21 (Blue)	2.1 (Magenta)	2 (Bluishgreen)
Lambda	0.006	0.001	0.0005

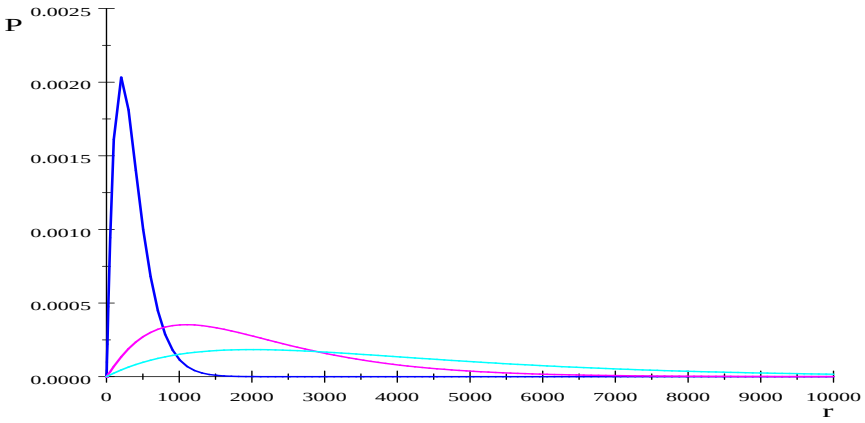

Figure 4. Distribution of cloud drops by drop size considering droplet in solution III.

REFERENCES

[1] W. Henry, Experiments on the quantity of gases absorbed by water, at different temperatures, and under different pressures, Phil. Trans. R. Soc. Lond., 93,1803,29-274.
[2] F.M. Raoult, The general law on the freezing of solvents,Ann. Chem. Phys. 2,1884,66-93.
[3] J.H. van't Hoff, The Role of Osmotic Pressure in the Analogy between solutions and gases, Zeitschrift fur physikalischeChemie 1, 1887, 481-508.
[4] B. J. Mason, The Physics of Clouds (Clarendon Press, Oxford, 1976).
[5] A.N. Matvéev, Física Molecular(Editorial Mir, Moscú, 1987).
[6] S. Lovejoy, D. Schertzer, Multifractals, Universality Classes and Satellite and Radar Measurements of Cloud and Rain Fields, Journal of Geophysical Research, vol. 95, No D3, 1990, 2021-2034.
[7] R.H. Riedi, I. Scheuring, Conditional and Relative Multifractal Spectra, Fractals, Vol. 5, No. 1,1997, 153-168.
[8] W. Thomson, W. On the size of atoms,Nature, 1,1870, 551–553.
[9] J.W. Gibbs, On equilibrium of heterogeneous substances, Trans. Connect. Acad., 3,1875-1876, 108–248.
[10] G.Arfken, Mathematical Methods for Physicists (2nd ed., Academic, New York,1985).
[11] E. Villermaux, Fragmentation, Annu. Rev. Fluid Mech., 39,2007, 419-446.
[12] A. Kokhanovsky, Cloud Optics (University of Bremen, Germany Published by Springer, Atmospheric and Oceanographic Sciences Library 34, Springer, 2006).

[13] R. Metzler, J. Klafter, The random walk's guide to anomalous diffusion: A fractional dynamics approach, Phys. Rep. 339, 2000, 1-77.
[14] A.I. Saichev, G.M. Zaslavsky, Fractional kinetic equations,Chaos 7 (4), 1997, 753-764.
[15] W.D.Bachalo, M.J. Houser, (1984), Phase/Doppler spray analyzer for simultaneous measurements of drop size and velocity distributions, Optical Engineering 23(5) 1984, 583 -590..
[16] A.R. Glover, S.M. Skippon and R.D. Boyle, Interferometric laser imaging for droplet sizing: a method for droplet-size measurement in sparse spray systems,Appl. Opt. 34, 1985, 8409–21
[17] R.A. Shaw, Particle-turbulence interactions in atmospheric clouds,Annual Review of Fluid Mechanics, 35(1), 2003, 183-227.
[18] J.R. Mercado-Escalante, W. Ojeda-Bustamante, P.A. Guido-Aldana y G. Zetina-Domínguez.Velocidad de sedimentación e interacciónfluido-partícula. Investigación en Matemáticas, Economía y Ciencias Sociales, Pág. 48-55.F. Pérez Soto, E. Figueroa Hernández, L. Godínez Montoya, R. M. García Núñez, D. Sepúlveda Jiménez, D. M. Santos Melgoza, (Compilación y Edición), Universidad Autónoma Chapingo, Primera edición, marzo de 2014, ISBN D.R. © Universidad Autónoma Chapingo,.
[19] J.R. Mercado-Escalante, P.A. Guido-Aldana, G. Zetina-Domínguez, Funnel Vortices and Fluid Particles Interaction, International Journal of Engineering Science and Innovative Technology (IJESIT), Vol. 4, Issue 3, May 2015, pp. 1-7.
[20] P. Banat, S.P. Malinowski, Properties of the turbulent cloud-clear air interface observed in the laboratory experiment,Physics and Chemistry of the Earth, Part B: Hydrology, Oceans and Atmosphere, 24(6),1999, 741-745.
[21] S.P. Malinowski, Turbulent mixing of a cloud with the environment: two-phase evaporating flow. Numerical simulations, laboratory experiments and field measurements,Journal of Theoretical and Applied Mechanics, 45(3),2007, 587-601.
[22] Z. Warhaft, Laboratory studies of droplets in turbulence: towards understanding the formation of clouds, Fluid Dyn. Res. 41, 2009.
[23] H.R. Pruppacher,J.D. Klett, Microphysics of Clouds and Precipitation: With an Introduction to Cloud Chemistry and Cloud Electricity, (Springer, New York, 1997).
[24] P. Götzfried, B. Kumar, R.A. Shaw and J. Schumacher, Droplet dynamics and fine-scale structure in a shearless turbulent mixing layer with phase changes, J. Fluid Mech. vol. 814,2017, pp. 452-483.
[25] S.P. Malinowski, I. Zawadzki I, P. Banat P., Laboratory Observations of Cloud–Clear Air Mixing at Small Scales,J. of Atmos. and Ocean. Techn. Volume 15, 1998, 1060-1066.
[26] H. Lian, G. Charalampous., Y. Hardalupas, Preferential concentration of poly-dispersed droplets in stationary isotropic turbulence, 16th Int. Symp. on Applications of Laser Techniques to Fluid Mechanics, Lisbon, Portugal, 2012.
[27] J.P. Salazar, J. De Jong, L. Cao, S.H. Woodward, H.Meng, &L.R. Collins, Experimental and numerical investigation of inertial particle clustering in isotropic turbulence, Journal of Fluid Mechanics, 600,2008, 245-256.
[28] B. De Sahagún B., Historia General de las Cosas de la Nueva España (Ed- Porrúa, 1956).
[29] D.L. Black, M.Q. McQuay, M.P. Bonin, Laser-based techniques for particle-size measurement: A review of sizing methods and their industrial applications. Prog. Energy Combust. Sci. Vol. 22,1996, pp. 267-306,
[30] P. Guido Aldana, G. May, E. Ramos. Application of the PIV technique to study the water droplets cloud dynamic in an energy tower model, 35 Congreso AIDIS y 59 Congreso ACODAL, Cartagena de Indias, Colombia, 2016.
[31] R.J. Schick, Spray Technology Reference Guide: Understanding Drop Size, Spraying Systems Co. Bulletin B, 459, 2006, 8-16.

AUTHORS BIOGRAPHY

José Roberto Mercado-Escalante. Independent Researcher, Mexico. Dr. of Sciences (Mathematics) by the National Autonomous University of Mexico-UNAM, Master Degree in Mathematics by the Autonomous University of Puebla-BUAP, graduates in Physics by the National University of Colombia. Research areas: inverse problems, fractals and fractional derivatives, physical and mathematical aspects of hydraulics. E-mail: jrmercadoe@yahoo.com

Pedro Antonio Guido-Aldana. Water Technology in the Mexican Institute of Water Technology – IMTA, Mexico. Affiliate to the Professional Development and Institutional Coordination. Doctorand Master in Hydraulic Engineering by the National Autonomous University of Mexico-UNAM, Civil Engineer by the University of the Coast, Barranquilla, Colombia. Associate Professor in the Engineering Faculty - UNAM. Research interest: water planning and management, climate change, potamology, river hydraulics, particle image velocimetry applications.E-mail: pedroguido@tlaloc.imta.mx

*José Roberto Mercado-Escalante " Fractal Description of Cloud Drops and Distribution According To Their Sizes" American Journal of Engineering Research (AJER) 6.8 (2017): 22-33